

# UC Irvine

## UC Irvine Previously Published Works

### Title

On the Hall Effect in Ferromagnetics

### Permalink

<https://escholarship.org/uc/item/3ft154dn>

### Journal

Physical Review, 82(1)

### ISSN

0031-899X

### Authors

Rostoker, N.  
Pugh, Emerson

### Publication Date

1951-04-01

### DOI

10.1103/PhysRev.82.125

Peer reviewed

in Fig. 2. The energy calibration was carried out by means of the  $K$ -radiation from Te. Figure 3 shows oscilloscope traces of the pulse distribution obtained from  $\text{Pa}^{231}$  in the proportional counter in comparison with the  $K$  x-rays emitted from  $\text{Te}^{126}$ . Critical absorption of the nuclear gamma-ray from  $\text{Pa}^{231}$  also showed that its energy lies between the absorption edges of Cd and In (26.7 and 27.9 kev) (Fig. 4). For this experiment, Cd, In, and Sn absorbers were placed between the sample and the beryllium window, and the discriminator voltage of the proportional counter was kept constant at the peak-value for the  $\gamma$ -ray. Teillac,<sup>6</sup> by means of a Wilson chamber technique, had observed at least 3 conversion electron groups from this isotope. The most intense group, at 24 kev, may be identified with the  $M$ -electrons from the 27-kev gamma-ray.

Low energy gamma-rays have hitherto received only scant attention. A systematic study of their occurrence is now in progress.

Our thanks are due to M. Studier of Argonne National Laboratory and G. Harbottle of this laboratory for the preparation of  $\text{Pa}^{231}$  samples, and to E. der Mateosian for valuable help.

- \* Research carried out under contract with AEC.  
<sup>1</sup> R. L. Macklin and G. B. Knight, Phys. Rev. 72, 435 (1947).  
<sup>2</sup> Scharff-Goldhaber, der Mateosian, McKeown, and Sunyar, Phys. Rev. 78, 325 (1950).  
<sup>3</sup> Compton and Allison, *X-Rays in Theory and Experiment* (D. Van Nostrand Company, Inc., New York, 1934).  
<sup>4</sup> Theory predicts only  $\sim 1L$  x-ray per  $10^4$   $\alpha$ -particles for this effect. Recent experiments on polonium show that this effect is of the order of 1 per  $10^3$  alphas [W. Rubinson and W. Bernstein, Bull. Am. Phys. Soc. 26, No. 1, 47 (1951)].  
<sup>5</sup> J. Teillac, Compt. rend. 239, 1056 (1950).  
<sup>6</sup> J. Teillac, Compt. rend. 229, 650 (1949).

## On the Hall Effect in Ferromagnetics

N. ROSTOKER AND EMERSON M. PUGH  
 Department of Physics, Carnegie Institute of Technology,  
 Pittsburgh, Pennsylvania  
 (Received January 18, 1951)

IN a recent paper,<sup>1</sup> hereafter referred to as (A), Hall effect measurements for nickel were presented. The following relation was proposed to describe the Hall effect on the basis of these measurements and previous measurements made by Smith<sup>2</sup>

$$e_H = R_0(H + 4\pi\alpha M), \quad (1)$$

where  $e_H$  is the Hall electric field per unit current density,  $R_0$  is the Hall constant which should depend chiefly on the numbers of electrons and holes and be substantially independent of temperature,  $H$  is the magnetizing force,  $M$  is the magnetization, and  $\alpha$  is a field parameter which increases with temperature. ( $\alpha$  varies from  $\alpha \sim 1$  at low temperatures to  $\alpha \sim 100$  in the neighborhood of the Curie point.)

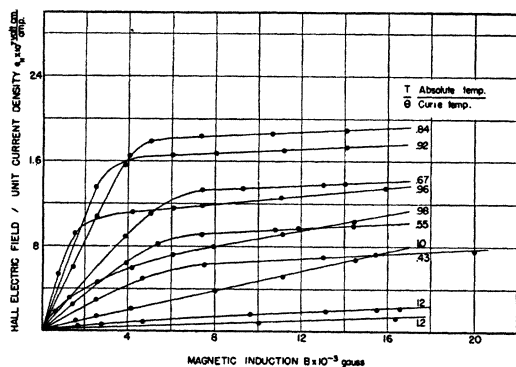


FIG. 1. Hall effect in nickel after A. W. Smith.

The experimental data of Smith are reproduced in Fig. 1. Here  $e_H$  has been plotted against  $B$ , the magnetic induction. It is clear that above technical saturation the slopes of  $e_H$  versus  $B$  curves are constant with increasing  $B$  and are essentially the same for different temperatures, except for the temperatures in the neighborhood of the Curie point where a sharp increase of these slopes with temperature is apparent. In (A),  $R_0$  was computed from these data with the assumption that above technical saturation  $M = \text{constant}$  with increasing  $B$  or  $H$ , so that:

$$R_0 = \partial e_H / \partial H = \partial e_H / \partial B. \quad (2)$$

The values of  $R_0$  thus computed from Smith's data are shown in Fig. 2, which corresponds to Fig. 3A of (A), and the "spike" in the neighborhood of the Curie point is very pronounced.

However, it has been discovered that, when the change in intrinsic magnetization with  $H$  after technical saturation is taken

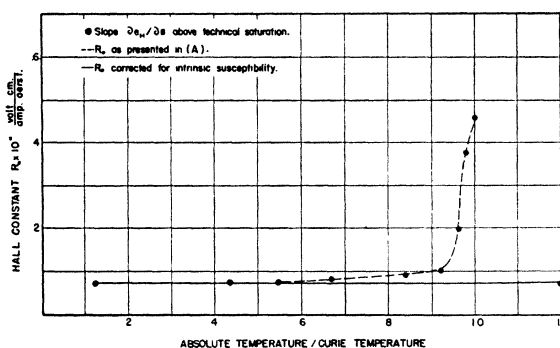


FIG. 2. Temperature dependence of the Hall constant  $R_0$  for nickel.

into consideration, the  $R_0$  versus  $T/\theta$  curve is altered as shown in Fig. 2 and the anomalous behavior in the neighborhood of the Curie point disappears. The behavior of the intrinsic magnetization for high field strengths in the case of nickel has been studied by Weiss and Forrer<sup>3</sup> over temperatures ranging from room temperature to well above the Curie point. A susceptibility  $\chi_i$  due to change in intrinsic magnetization at high field strengths can be estimated from their data:

$$\chi_i = \partial M / \partial H. \quad (3)$$

At room temperature, we find  $\chi_i \sim 1.7 \times 10^{-4}$ , which is so small that it does not significantly alter our previously computed value of  $R_0$ . The only significant change occurs near the Curie point, where  $\chi_i$  is much larger. For example, in the neighborhood of the paramagnetic Curie point  $\theta$ ,  $\chi_i \sim 3.7 \times 10^{-3}$ .

From Eq. (1)  $\partial e_H / \partial H = R_0(1 + 4\pi\alpha\chi_i)$  and, since  $\partial e_H / \partial H = (1 + 4\pi\alpha\chi_i)\partial e_H / \partial B$ ,

$$R_0 = [(1 + 4\pi\alpha\chi_i) / (1 + 4\pi\alpha\chi_i)] \partial e_H / \partial B. \quad (2.1)$$

Equation (2.1) reduces to Eq. (2) when  $\chi_i$  is small, which is the case in the neighborhood of the Curie point. When  $R_0$  was computed by the more correct Eq. (2.1), using the experimental data of Weiss and Forrer, it was found that Eq. (1) is consistent with the experimental data of Smith and Schindler presented in (A), with  $R_0$  a constant independent of both temperature and magnetic fields, and with  $\alpha$  a parameter dependent on temperature only.

It was previously suggested<sup>4</sup> by one of us that Eq. (1) might be applicable to paramagnetic as well as ferromagnetic substances, but that it might be difficult to detect the contribution to the Hall effect from the magnetization in most paramagnetic substances, because the magnetization is proportional to  $H$  and very small. The above discussion indicates an observable paramagnetic contribution to the Hall effect in nickel in the neighborhood of the Curie point where the nickel is strongly paramagnetic.

By properly separating the extraordinary Hall effect due to magnetization from the ordinary Hall effect due to a uniform field (the magnetizing force  $H$ ), a well-behaved Hall constant for ferromagnetics can be measured which should provide considerable information concerning the band structure of ferromagnetics.

<sup>1</sup> Pugh, Rostoker, and Schindler, Phys. Rev. **80**, 688 (1950).

<sup>2</sup> A. W. Smith, Phys. Rev. **30**, 1 (1910).

<sup>3</sup> P. Weiss and R. Forrer, Ann. phys. **5**, 153 (1926).

<sup>4</sup> E. M. Pugh, Phys. Rev. **36**, 1503 (1930).

## Scattering of 20-Mev Alpha-Particles by Helium

K. B. MATHER\*

Physics Department, Birmingham University, Birmingham, England\*\*

(Received February 9, 1951)

THE angular distribution of alphas elastically scattered from helium gas has been studied using a photographic method. Twenty-Mev alphas from the cyclotron entered the scattering chamber from a collimating slit system. Scattering angles were defined by a number of radial slots (Fig. 1) cut in an iron ring, each

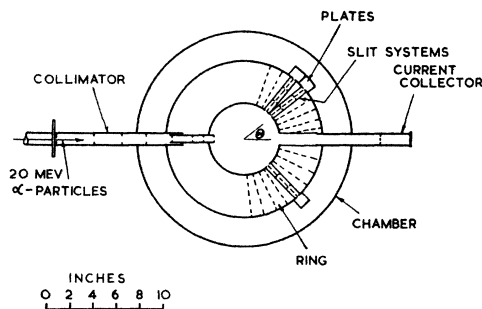


FIG. 1. Schematic of photographic scattering chamber. Angles of scattering are defined by the slits mounted in radial slots cut in the ring (dotted lines indicate positions of slit systems).

mounting a set of defining slits. Particles scattered through these slits were recorded by their tracks in photographic emulsions placed at known angles behind each slot.

The scattering cross section  $\sigma(\Theta)$  at any laboratory angle  $\Theta$ , could be calculated from measurements of slit dimensions, slit distances from the scattering volume, angles of tilt of the photographic plates to the horizontal, the total number of alphas traversing the chamber, and the number of tracks per unit area of plate surface. A noteworthy advantage of the chamber was its dependence predominantly on length measurements which could be made easily and accurately. The number of particles traversing the chamber was determined by collecting the total charge on a Faraday cup connected to a 1.10- $\mu$ f condenser whose potential was measured with a calibrated quadrant electrometer. The helium gas pressure was obtained from an Apiezon B oil manometer.

The alpha-particle energy was ascertained by measuring the ranges in photographic emulsions of the alphas at each angle of scattering  $\Theta$ ;  $E_0 = 20.0 \pm 0.3$  Mev.

The data reported here is preliminary only, being based on a single run and with a total track count of only  $\sim 7000$ . Owing to the small alpha-beams produced by the cyclotron; runs were very long, which resulted in trouble from impurity scattering, leakage corrections to the current integrator system, and relatively poor statistics. In proton scattering it is feasible to apply reliable corrections for impurity scattering (air and vapors) based on identifiably different *bona fide* and spurious track lengths. This feature is almost lost in alpha-scattering because of the less favorable mass ratio between scattered and impurity particles.

Table I lists  $\sigma(\theta)$ , the center-of-mass scattering cross section versus center-of-mass angle  $\theta$ , together with probable errors based

TABLE I. Center-of-mass cross sections  $\sigma(\theta)$  for 20-Mev alpha-alpha scattering, and ratio to Mott cross sections.

$\Theta$	$\theta$	$\sigma(\theta) \times 10^{26}$ cm <sup>2</sup> sterad <sup>-1</sup>	$\frac{\sigma_{\text{obs}}}{\sigma_{\text{Mott}}}$
7°	14°	*14.1 ± 0.7	1.53
11	22	* 7.7 0.3	4.85
15	30	3.9 0.1	7.82
16	32	3.7 0.1	9.34
21	42	2.00 0.11	12.8
25	50	1.58 0.06	17.3
30	60	1.23 0.08	21.9
35	70	0.92 0.06	22.4
40	80	1.04 0.07	30.4
45	90	—	—
50	100	0.97 0.08	28.4
55	110	1.06 0.08	25.9
60	120	1.19 0.09	21.2

on the statistics at each angle. By comparison, other errors which affect the relative cross sections are negligible at most angles. However, absolute values of  $\sigma(\theta)$  may be in error by as much as 10 percent. The starred values are very uncertain owing to impurity effects at small angles. (They probably can be taken as upper limits.) Column 4 gives the ratio of observed to Mott cross sections:

$$\sigma(\theta)_{\text{Mott}} = \frac{4e^4}{E_0^2} [\text{cosec}^4\Theta + \sec^4\Theta + 2 \text{cosec}^2\Theta \cdot \sec^2\Theta \cdot \cos(\eta \log \tan^2\Theta)]$$

$$\eta = 4e^2/\hbar v = 0.282 \text{ for 20-Mev alphas.}$$

As expected, there was no evidence at 20 Mev of inelastic scattering. However, if the alpha-particle has excited states 10 to 20 Mev above ground, an alpha-alpha experiment at 40 Mev could (at least from energy considerations) show inelastic scattering. It is proposed to attempt this with alphas from the Birmingham 60-in. cyclotron.

\* Temporarily with the University of Ceylon, Colombo, Ceylon.

\*\* Exposures were made at Washington University, St. Louis, Missouri, in 1949, using the 45-in. cyclotron.

## The Discrepancy in the Energy of Annihilation Radiation and the Possibility of Electron-Positron Mass Difference

ARNE HEDGRAN AND DAVID A. LIND\*  
Nobel Institute of Physics, Stockholm, Sweden  
January 20, 1951

THE energies of certain gamma-radiations (Au<sup>198</sup>, Co<sup>60</sup>, and annihilation radiation) have been measured with good precision with a crystal spectrometer.<sup>1</sup> Recently, however, it became apparent from measurements on the double focusing spectrometer<sup>2</sup> at this laboratory that there was a discrepancy between the energy of the annihilation radiation measured in terms of the Au<sup>198</sup> 411-kev line and the value calculated from the Einstein relation  $E_0 = m_0c^2$  using the best values of the constants.<sup>3</sup>

The comparison of the Au<sup>198</sup> radiation with the annihilation radiation can be made very accurately because electrons ejected from the  $L_{III}$  shell in uranium by the 411-kev radiation have a momentum only 1 part in 1000 less than those ejected from the  $K$  shell by the annihilation radiation. The effect of converter thickness is the same for both lines; it is necessary to consider only the effect of the Doppler broadening.

Comparisons were carried out with sources of Au<sup>198</sup>, Cu<sup>64</sup>, and Co<sup>60</sup> mounted in brass tubes to eliminate the continuous beta-spectra. The positrons from the Cu<sup>64</sup> annihilate in copper or brass. A 0.7-mg/cm<sup>2</sup> uranium converter was used and the resolution set at  $1.6 \times 10^{-3}$ . For comparison, window curves for thorium  $I$ ,  $L$ , and  $X$  lines at 1750, 2603, and 10,000  $H\rho$ , respectively, were also taken. These were used to correct for the converter effects.

The shapes of the Au<sup>198</sup>  $UL_{III}$  and Cu<sup>64</sup>  $U_K$  lines, shown as curves  $A$  and  $C$ , respectively, in Fig. 1, were obtained by a suitable